

The wave-packet approach to shot noise in double barrier resonant diodes: a way to distinguish coherent from sequential tunneling

V. Ya. Aleshkin

Institute for Physics of Microstructures, Nizhny Novgorod GSP-105 603600, Russia

L. Reggiani

National Nanostructure Laboratory of INFM, Dipartimento di Ingegneria dell' Innovazione, Università di Lecce, Via Arnesano s/n, 73100 Lecce, Italy

N.V. Alkeev, V.E. Lyubchenko

Institute of Radioengineering & Electronics, Russian Academy of Sciences

C.N. Ironside, J.M.L. Figueiredo and C.R. Stanley

Department of Electronic and Electrical Engineering, University of Glasgow

(Dated: May 22, 2019)

The wave-packet approach originally developed by Martin and Landauer (Phys. Rev. B45, 1742, 1992) is implemented to include long range Coulomb interaction and applied to investigate current voltage characteristics and shot noise in double barrier resonant diodes. Theory is based on a coherent approach and covers the region of low applied voltages up to the region of the current peak. The shape of the current voltage characteristic is well reproduced and we predict that shot noise can be suppressed with a Fano factor well below the value of 0.5. This feature is a signature of coherent tunnelling since the standard sequential tunnelling predicts in general a Fano factor equal to or greater than the value 0.5. This giant suppression of shot noise can occur at zero temperature as a consequence of Pauli principle as well as at high temperatures above about 77 K as a main consequence of long range Coulomb interaction. The theory is found to be in quantitative agreement with experimental data.

PACS numbers: PACS numbers: 72.70.+m, 72.20.-i, 72.30+a, 73.23.Ad

I. INTRODUCTION

Since its realization¹, the double barrier resonant diode (DBRD) proved to be an electron device of broad physical interest because of its peculiar non Ohmic current voltage (I-V) characteristic. Indeed, after a strong super-Ohmic increase of current it exhibits a negative differential conductance and eventually hysteresis effects.² Even the shot noise characteristics of DBRDs are of relevant interest in the sense that suppressed as well as enhanced shot noise with respect to the full Poissonian value has been observed (see Ref. [3] for a review on the subject). These electrical and noise features are controlled by the mechanism of carrier tunneling through the double potential barriers. The microscopic interpretation of these features is found to admit a coherent or a sequential tunneling approach³. The coherent approach⁴ consists in considering the whole device as a single quantum system characterized by a transmission coefficient describing carrier transport from one contact to the other. By contrast, the sequential approach⁵ consists in considering tunneling through the diode as a two step process where carriers first transit from one contact into the well, then from the well to the other contact. The intriguing feature of these two approaches is that from the existing literature it emerges that both of them are capable to explain the

I-V experimental data as well as most of the shot noise characteristics. Therefore, to our knowledge there is no way to distinguish between these two transport regimes and the natural question whether the tunnelling transport is coherent or sequential remains an unsolved one.

The coherent approach to shot noise in DBRD has received wide attention since the first experimental evidence by Li et al⁶ of shot noise suppression with a minimum value of the Fano factor $\gamma = S_I/(2qI) = 0.5$, here S_I is the low frequency spectral density of current fluctuations and q the absolute value of the unit charge responsible of current. Remarkably, most of the coherent approaches developed so far^{7,8,9,10,11,12} predict a maximum suppression $\gamma = 0.5$ even if there is clear experimental evidence of suppression below this value^{8,13,14} down to values of $\gamma = 0.25$.^{13,14} To this purpose, some authors obtained theoretical values of the Fano factor just below the value of 0.5, Ref. [15] found 0.45 and Ref. [16] 0.38, respectively. However, the physical interpretation of these results remains mostly qualitative and quoting Ref. [3] this direction of research looks promising but certainly requires more efforts. We remark that the theory of shot noise in DBRDs under the sequential approach^{11,15,17,18,19,20,21,22,23,24} provides a Fano factor of 0.5 as the minimum value of shot noise suppression.

The aim of this paper is to develop a coherent theo-

retical approach for current voltage and electronic noise in DBRDs accounting for Pauli principle and long range Coulomb interaction going beyond existing models. To this purpose, we implement the wave-packet approach originally proposed in Refs. [25,26] by including the effect of long range Coulomb interaction and applying it to DBRDs. We anticipate that the main result of the present theoretical approach concerns with the prediction that suppression of shot noise with a Fano factor below 0.5 is a signature of coherent tunneling against sequential tunneling. Such a prediction is confirmed by experimental results.

The content of the paper is organized as follows. Section 2 presents the theoretical model. Section 3 provides the analytical expressions for the calculation of the current voltage characteristics in the low voltage region limited to the first peak of the current. Section 4 provides the analytical expression for the electron noise corresponding to the current voltage characteristics of Sect. 2. Here, the Nyquist expression is recovered at vanishing applied voltage. At increasing voltage suppressed shot noise is found in the region preceding the current peak and enhanced shot noise at voltages just above the current peak. Section 5 reports a comparison between theory and existing experiments. Major conclusions are drawn in Sect. 6.

II. MODEL

The typical diode investigated here is the standard symmetric double well structure depicted in Fig. 1. We denote by $\Gamma = (\Gamma_L + \Gamma_R)$ the resonant states width and by ε_r the energy of the resonant level as measured from the center of the potential well and $\Gamma_{L,R}$ the partial widths due to the tunnelling through the left and the right barrier, respectively. We consider the case of coherent tunnelling in the presence of only one resonant state and we assume that the diode has contacts with unit square surfaces. For convenience calculations are carried out using the cgs system.

The kinetic model is developed by assuming that the electron distribution functions in the emitter and in the collector, f_i , are equilibrium-like, but with different electro-chemical potentials F_i :

$$f_i(\varepsilon, F_i) = \frac{1}{1 + \exp\left(\frac{\varepsilon - F_i}{k_B T}\right)}, \quad (1)$$

here $i = L$ stands for the left contact (the emitter), $i = R$ for the right contact (the collector), k_B is the Boltzmann constant, T the bath temperature and ε the kinetic carrier energy.

Following Blanter and Büttiker²², we introduce an effective longitudinal density of states for the resonant level, G_{QW} , which corresponds to the Breight-Wigner²⁷

limit for the resonant tunneling:

$$G_{QW}(\varepsilon_z) = \frac{\Gamma}{2\pi\Gamma_L\Gamma_R} D(\varepsilon_z) \quad (2)$$

with the transparency of the double barrier $D(\varepsilon_z)$ given by

$$D(\varepsilon_z) = \frac{\Gamma_L\Gamma_R}{(\varepsilon_z - \varepsilon_r + qu)^2 + \frac{\Gamma^2}{4}}$$

where $-q$ is the electron charge, u the voltage drop between the emitter and the center of the potential well, ε_z the carrier energy of the longitudinal motion (see Fig. 1).

The electron flux from the resonant state to the emitter and the collector, $R_{L,R}$, respectively, can be written in the following form²³:

$$R_{L,R} = \frac{m\Gamma_{L,R}}{\pi\hbar^3} \int_{-g_{L,R}}^{\infty} d\varepsilon_z G_{QW}(\varepsilon_z) \int_0^{\infty} d\varepsilon_{\perp} f_{QW}(\varepsilon) \times [1 - f_{L,R}(\varepsilon)] \quad (3)$$

where m is the electron effective mass, ε_{\perp} the kinetic energy of the transverse motion, $\varepsilon = (\varepsilon_z + \varepsilon_{\perp})$, g_L (u_L) the energy gap between the bottom of the conduction band and the first quantization level in the well before the left barrier (see Fig. 1), $g_R = qV$, u_L the potential drop in the emitter, V the total applied voltage, $f_{QW}(\varepsilon)$ the distribution function inside the quantum well. Analogously, the electron flux to the quantum well from the emitter and the collector, $G_{L,R}$, respectively, are written as²³:

$$G_{L,R} = \frac{m\Gamma_{L,R}}{\pi\hbar^3} \int_{-g_{L,R}}^{\infty} d\varepsilon_z G_{QW}(\varepsilon_z) \int_0^{\infty} d\varepsilon_{\perp} f_{L,R}(\varepsilon) \times [1 - f_{QW}(\varepsilon)] \quad (4)$$

In our model, we suppose that in the emitter there are no electron states with energy below $-g_L$ and that electron states with energy higher than this value are three dimensional. Under stationary conditions, the sum of the incoming and the outgoing fluxes are equal for each ε_z , ε_{\perp} independently. From this condition we find that the distribution function in the quantum well is given by:

$$f_{QW}(\varepsilon) = \frac{\Gamma_L}{\Gamma} f_L(\varepsilon) + \frac{\Gamma_R}{\Gamma} f_R(\varepsilon) \quad (5)$$

when there are fluxes to the quantum well from the emitter and the collector, and:

$$f_{QW}(\varepsilon) = f_R(\varepsilon) \quad (6)$$

when there is only flux from the collector. We note that under coherent tunneling the time necessary to establish Eq. (5) under the response of the system to an external step-like perturbation is of the order of \hbar/Γ^{28} . Accordingly, we shall discuss the situation when the characteristic time scale of any voltage change is sufficiently longer than \hbar/Γ so that Eqs. (5) and (6) are always valid. Of course, under thermal equilibrium conditions it is: $f_L(\varepsilon) = f_R(\varepsilon) = f_{QW}(\varepsilon)$.

III. CURRENT VOLTAGE CHARACTERISTICS

By making use of Eqs. (3) to (5) we obtain the well known expression for the electron current from the emitter to the collector in the resonant tunneling diode²³:

$$I = -q(G_L - R_L) = \frac{-qm}{2\pi^2\hbar^3} \int_{-g_L}^{\infty} D(\varepsilon_z) d\varepsilon_z \times \int_0^{\infty} d\varepsilon_{\perp} [f_L(\varepsilon) - f_R(\varepsilon)] \quad (7)$$

To determine the transparency explicitly we must find $u_L(V)$ and $u(V)$ as functions of the total applied bias V . To this purpose, we consider the Poisson equation for the electrical potential φ in the resonant barrier structure of Fig. 1. In the emitter the Poisson equation can be written in the form

$$\varphi'' = \frac{4\pi q}{\kappa} \left[N_c F_{1/2} \left(\frac{F_L + q\varphi}{k_B T} \right) - n \right] \quad (8)$$

with

$$n = N_c F_{1/2} \left(\frac{F_L}{k_B T} \right)$$

the electron concentration in the emitter, N_c the effective density of states of the conduction band, $F_{1/2}(x)$ the Fermi-Dirac integral of index 1/2²⁹, κ the static dielectric constant of the material. We note that the effect of size quantization on the electron distribution in the emitter has been neglected. By integrating Eq. (8) and taking into account that $\varphi(-\infty) = \varphi'(-\infty) = 0$, we find the relation between φ'_L and u_L on the left border of the left barrier

$$\varphi'_L = \sqrt{\frac{8\pi k_B T}{\kappa}} \times \left[N_c F_{3/2} \left(\frac{F_L + qu_L}{k_B T} \right) - N_c F_{3/2} \left(\frac{F_L}{k_B T} \right) - \frac{q}{k_B T} n u_L \right]^{1/2} \quad (9)$$

Here $F_{3/2}$ is the Fermi-Dirac integral of index 3/2.²⁹ To simplify the task, we suppose that the barriers are undoped and that the charge of the quantum well is placed at its middle plane, so that we can write

$$u = u_L + \varphi'_L (d_L + d_{QW}/2) \quad (10)$$

and

$$u_R = u + \left(\varphi'_L - \frac{4\pi}{\kappa} Q_{QW} \right) (d_R + d_{QW}/2) \quad (11)$$

with d_L , d_R , d_{QW} the widths of the left barrier, right barrier, and quantum well, respectively; $Q_{QW} =$

$q(N_{QW}^+ - N_{QW})$ is the charge in the quantum well; N_{QW}^+ and N_{QW} are the number of charged donors and electrons in the quantum well

$$N_{QW} = \frac{m}{\pi\hbar^2} \int_0^{\infty} d\varepsilon_{\perp} \left[\int_{-g_L}^{\infty} d\varepsilon_z G_{QW}(\varepsilon_z) \left(\frac{\Gamma_L}{\Gamma} f_L(\varepsilon) + \frac{\Gamma_R}{\Gamma} f_R(\varepsilon) \right) + \int_{-qV}^{-g_L} d\varepsilon_z G_{QW}(\varepsilon_z) f_R(\varepsilon) \right] \quad (12)$$

Note that we have chosen $-qV$ instead of $-qu_R$ as lower limit of the second integral in the right hand side of Eq. (12). This is a good approximation due to the fast decrease with energy of $G_{QW}(\varepsilon)$. Furthermore, we suppose that the electron concentration in the collector is the same of that in the emitter, hence $F_R = F_L - qV$ and the Poisson equation in the collector takes the form given by Eq. (8) with the change $F_L \rightarrow F_R$. By integrating this new equation with the condition $\varphi(\infty) = V$, $\varphi'(\infty) = 0$, in analogy with Eq. (9), we obtain

$$-\frac{k}{4\pi} \varphi'_L + Q_{QW} + \frac{k}{4\pi} \sqrt{\frac{8\pi k_B T}{\kappa}} \left[N_c F_{3/2} \left(\frac{F_L + qu_R - qV}{k_B T} \right) - N_c F_{3/2} \left(\frac{F_L - qV}{k_B T} \right) - \frac{qn}{k_B T} (u_R - V) \right]^{1/2} = 0 \quad (13)$$

Equation (13) relates u_R to V . We remark that it is more convenient to consider V and I as functions of u_L because in this case they are single valued functions even for I-V characteristics of Z-type. Since the first and the third term in the left hand side of Eq. (13) are the charge of the emitter Q_L and of the collector Q_R , respectively, Eq. (13) expresses the condition of electroneutrality of the device. We note that, to derive Eq. (13) we have assumed that the width of the depletion region in the collector region (see Fig. 1) is smaller than that between the right barrier and the highly doped region in the collector. As typical in DBRs, from both sides of the barriers there are spacers with doping level of the order of $10^{16} \div 10^{17} \text{ cm}^{-3}$ with widths from several tens⁸ to several hundreds³⁰ of nanometer. If the low doped region in the collector is fully depleted, then we must change Eq. (13) with

$$V = u_R + \varphi'_R L - \frac{2\pi q n L^2}{\kappa} \quad (14)$$

here L is the width of the spacer in the collector, and $\varphi'_R = \varphi'_L - 4\pi Q_{QW}/\kappa$. In the derivation of Eq. (14) the voltage drop in the highly doped collector region has been neglected.

IV. NOISE

To calculate the noise we use the wave-packet approach suggested by Landauer²⁵ and detailed by Martin and

Landauer²⁶. In this approach, electrons in the energy interval $\Delta\varepsilon_z$ are sent from a given lead to the sample region one at a time, at a rate $1/\tau$ with $\tau = 2\pi\hbar/\Delta\varepsilon_z$. By denoting the current associated with a single electron wave packet by $j_{s,k_\perp}(t)$, the total current as superposition of orthogonal wave-packets shifted in time, is

$$I(t) = \sum_{k_\perp} \sum_n j_{k_\perp}(t - n\tau) g_n \quad (15)$$

with \mathbf{k}_\perp the wavevector component perpendicular to the z -direction (i.e. to the barriers), the sum over $n = 1, 2, 3, \dots$ is extended to the number of packets during the observation time,

$$j_{k_\perp}(t) = j_{s,k_\perp}(t) + \delta I_{n,k_\perp}(t) \quad (16)$$

and where: g_n equals $+1$ if the pulse is transmitted to the right (i.e. to the collector), or -1 if the pulse is transmitted to the left (i.e. to the emitter), and $\delta I_{n,k_\perp}$ is the fluctuation of the total current due to the space charge. The space charge, in turn, controls the change of transparency in other channels (with different \mathbf{k}_\perp and ε_z) due to j_{s,k_\perp} as it was already noted in Ref. [8]. We remark that, in analogy with the case of vacuum diodes³¹, $\delta I_{n,k_\perp}$ arises while the pulse j_{s,k_\perp} creates deviations from its average value of the charge in the quantum well. Following Ref. [26], we obtain the following expression for the spectral density of current fluctuations at zero frequency

$$S_I(0) = \frac{q^2 m}{\pi^2 \hbar^3} \int d\varepsilon_\perp \int d\varepsilon_z \langle q_{eff}^2 g^2 - \langle g \rangle^2 \rangle \quad (17)$$

where brackets denote ensemble average. In equation (17), $q_{eff} = j_\omega(0)/q$, with $j_\omega(0)$ the Fourier transform of $j_{k_\perp}(t)$ for $\omega = 0$, is a dimensionless effective charge which accounts for space charge effects when its value differs from unity. To justify Eq. (17) it is sufficient that all pulses j_{s,k_\perp} are *independent* from each other, what is valid for coherent tunneling.

Now we evaluate explicitly q_{eff} , $\langle g \rangle$, and $\langle g^2 \rangle$. To calculate of q_{eff} , we consider that there are two pulse histories which provide current for a given energy²⁶, namely: (i) when an electron from the emitter goes to the collector, (ii) when an electron from the collector goes to the emitter.

In history (i), the electron state in the emitter is occupied and that in the collector is empty. The probability of this process is $D(\varepsilon_z) f_L(\varepsilon) [1 - f_R(\varepsilon)]$. Let us choose $\Delta\varepsilon_z$ to be much smaller than Γ so that the condition $\tau \gg \hbar/\Gamma$ is satisfied. In this way the single wave-packet is very spread out in space and its transmission time is much longer than \hbar/Γ . From Eq. (7), and taking into account that $f_L = 1$ and $f_R = 0$, we obtain the following expression for the current density associated with the electron jump connected with $j_{s,k_\perp}(t)$

$$j_1 = -q D(\varepsilon_z) \frac{\Delta\varepsilon_z}{\pi\hbar} \quad (18)$$

By definition, the integral over time of $j_{s,k_\perp}(t)$ is equal to $-q$ which, in turn, can be written as the product between j_1 and a transit time $\tau_t(\varepsilon_z)$. Thus, we obtain

$$\tau_t(\varepsilon_z) = \frac{\pi\hbar}{D(\varepsilon_z) \Delta\varepsilon_z} \quad (19)$$

To find q_{eff} for this pulse history we note that, under fixed total voltage, the total current is function of u_L and, therefore,

$$\delta I_n(t) = \frac{\partial I_n}{\partial u_L} \delta u_L(t) \quad (20)$$

where $\delta u_L(t)$ is the fluctuation of the voltage drop u_L due to the pulse $j_{s,k_\perp}(t)$ that is determined as follows. Let δN_{QW} be the fluctuation of the total number of electrons in the quantum well due to a single electron pulse, then we can write:

$$\delta N_{QW} = \delta n_{QW} + \frac{\partial N_{QW}}{\partial u_L} \delta u_L \quad (21)$$

where in the right hand side of Eq. (21) the first term is associated with the fluctuations due to the distribution function and the second term with the fluctuations due to the electrical potential associated with long range Coulomb interactions. According to Eq. (12), δn_{QW} is given explicitly by

$$\delta n_{QW}(\varepsilon) = \frac{\Gamma_L [1 - f_L(\varepsilon)] - \Gamma_R f_R(\varepsilon)}{\pi \Gamma_L \Gamma_R} D(\varepsilon_z) \Delta\varepsilon_z \quad (22)$$

which represents the fluctuation number of electrons in the channel associated with the single electron pulse (we recall that during the pulse it is $f_L = 1$ and $f_R = 0$ what differs from the average value of $f_{L,R}$ and is the reason for the appearance of δu_L). By differentiating Eq. (13) we find the interrelations:

$$\delta Q_L + \delta Q_{QW} + \delta Q_R = 0, \quad C_L \delta u_L + q \delta N_{QW} + C_R \delta u_R = 0 \quad (23)$$

where $C_{L,R} = -\partial Q_{L,R}/\partial u_{L,R}$ ($V = const$) are the differential capacitances whose expressions are detailed in the Appendix (we note that when Eq. (14) is valid it is $C_R = \kappa/(4\pi L)$). By using Eq. (11) and the definition of C_L we find

$$\delta u_R = \delta u_L \left(1 + \frac{C_L}{C_1} \right) + \frac{q \delta N_{QW}}{C_2} \quad (24)$$

where

$$C_1 = \frac{\kappa}{4\pi (d_L + d_R + d_{QW})}, \quad C_2 = \frac{\kappa}{4\pi (d_R + d_{QW}/2)} \quad (25)$$

From Eqs. (23) and (24) we obtain

$$\delta N_{QW} = -\delta u_L \frac{C}{q} = -\delta u_L \frac{C_L + C_R (1 + C_L/C_1)}{q (1 + C_R/C_2)} \quad (26)$$

From Eqs. (21), (22) and (26) we obtain

$$\delta u_L = -\frac{q\delta n_{QW}}{C + q\frac{\partial N_{QW}}{\partial u_L}} \quad (27)$$

By using Eqs. (19) and (20) we can write the expression for the integral over time of δI_n

$$\int \delta I_n dt = -\frac{q\delta n_{QW}}{C + q\frac{\partial N_{QW}}{\partial u_L}} \left(\frac{\partial I}{\partial u_L} \right) \tau_t = -\frac{q\hbar [\Gamma_L (1 - f_L(\varepsilon)) - \Gamma_R f_R(\varepsilon)]}{\Gamma_L \Gamma_R \left(C + q\frac{\partial N_{QW}}{\partial u_L} \right)} \left(\frac{\partial I}{\partial u_L} \right) \quad (28)$$

which finally implies for q_{eff}^+ the expression:

$$q_{eff}^+(\varepsilon) = -1 - \frac{\hbar [\Gamma_L (1 - f_L(\varepsilon)) - \Gamma_R f_R(\varepsilon)]}{\Gamma_L \Gamma_R \left(C + q\frac{\partial N_{QW}}{\partial u_L} \right)} \frac{\partial I}{\partial u_L} \quad (29)$$

For the pulse history (ii), the electron state in the emitter is empty and that in the collector is occupied. The probability of this process is $D(\varepsilon_z) f_R(\varepsilon) [1 - f_L(\varepsilon)]$ which implies

$$\delta n_{QW} = \frac{\{\Gamma_R [1 - f_R(\varepsilon)] - \Gamma_L f_L(\varepsilon)\}}{\pi \Gamma_L \Gamma_R} D(\varepsilon_z) \Delta \varepsilon_z \quad (30)$$

By using Eq. (18), and (30) and taking into account that here the integral over time of $j_{s,k_\perp}(t)$ equals q , for the effective charge of this process we find:

$$q_{eff}^-(\varepsilon) = 1 - \frac{\hbar [\Gamma_R (1 - f_R(\varepsilon)) - \Gamma_L f_L(\varepsilon)]}{\Gamma_L \Gamma_R \left(C + q\frac{\partial N_{QW}}{\partial u_L} \right)} \frac{\partial I}{\partial u_L} \quad (31)$$

By taking into account that by definition

$$\langle g(\varepsilon) \rangle = D(\varepsilon_z) [f_L(\varepsilon) - f_R(\varepsilon)] \quad (32)$$

and that following Ref.[26]

$$\langle q_{eff}^2(\varepsilon) g^2(\varepsilon) \rangle = q_{eff}^{+2}(\varepsilon) D(\varepsilon_z) f_L(\varepsilon) (1 - f_R(\varepsilon)) +$$

$$q_{eff}^{-2} D(\varepsilon_z) f_R(\varepsilon) (1 - f_L(\varepsilon)) \quad (33)$$

Equation (17) takes the explicit form:

$$S_I(0) = \frac{q^2 m}{\pi^2 \hbar^3} \int_0^\infty d\varepsilon_\perp \int_{g_L}^\infty d\varepsilon_z \{ D[q_{eff}^+]^2 f_L (1 - f_R) +$$

$$(q_{eff}^-)^2 f_R (1 - f_L) - D^2 (f_L - f_R)^2 \} \quad (34)$$

Equation (34) is the central result of this paper. When $|q_{eff}^\pm| = 1$, Eq. (34) coincides with the expression derived in Ref. [26]. We remark that Ref. [8], by assuming

that the current component fluctuations are Poissonian distributed, did not account properly for Fermi statistics which implies binomial distribution, thus obtaining not accurate results. As an internal check now we demonstrate that Eq. (34) satisfies Nyquist theorem. Indeed, at zero applied voltage $f_L = f_R$ and it is easy to see from the expression for the total current in Eq. (7) that in this case $\partial I / \partial u_L = 0$ and $|q_{eff}^\pm| = 1$. Thus, Eq. (34) recovers the formula given in Ref. [26] which was there proven to satisfy the Nyquist theorem, and this concludes the demonstration.

Let us now show that $S_I(0) \rightarrow \infty$ on the border of the instability region where $dI/dV \rightarrow \infty$. To this purpose, we note that the full derivative dI/dV can be expressed in the form:

$$\frac{dI}{dV} = \frac{\partial I}{\partial V} + \frac{\partial I}{\partial u_L} \frac{du_L}{dV} \quad (35)$$

From Eq. (13) we have

$$C_L du_L + q dN_{QW} + C_R (du_R - dV) = 0 \quad (36)$$

By taking into account Eq. (23) and that

$$dN_{QW} = \frac{\partial N_{QW}}{\partial u_L} du_L + \frac{\partial N_{QW}}{\partial V} dV \quad (37)$$

from Eq. (24) and (36) we obtain

$$\frac{du_L}{dV} = \frac{C_R (1 + C_R/C_2)^{-1} - q \frac{\partial N_{QW}}{\partial V}}{\left(C + q \frac{\partial N_{QW}}{\partial u} \right)} \quad (38)$$

By using Eq. (7) for I , we see that $\partial I / \partial u_L$ and $\partial I / \partial V$ entering Eq. (35) are always finite. It implies that $dI/dV \rightarrow \infty$ only if the denominator in Eq. (38) goes to zero. We note that also Eqs. (29) and (31) for q_{eff}^\pm have the same denominator; thus, the effective charges and as a consequence $S_I(0)$ go to infinity simultaneously with dI/dV .

V. RESULTS AND DISCUSSION

In this section we will present in details the theoretical results for the two relevant cases of zero and high temperatures (i.e. $T \geq 77$ K), the former being appropriate to investigate the influence of the Pauli principle and the latter the influence of long range Coulomb interaction on the shot noise. Then, the present theory is compared with experiments.

A. Zero temperature

In this case, only the states for which $f_L = 1$ and $f_R = 0$ take part to the current transmission. Under these conditions, from Eq. (22) we see that $\delta n_{QW} = 0$ and hence $q_{eff}^+ = 1$. Thus, as expected Coulomb interaction

is washed out at zero temperature. This result is valid at any voltage with the exception of the voltage values near to the border of the stability region where dI/dV and $q_{eff}^+ \rightarrow \infty$. Let us investigate the case of high applied voltages, when $qV > F_L$, because it is more close to experiments. (We recall that typical magnitude for the relevant parameters of the DBRDs are: for Γ less than a few meV, for F_L less than 100 meV, and for the applied voltage at the peak current around 0.5 V.) Because of the above, Eq. (34) takes the form

$$S_I(0) = \frac{q^2 m}{\pi^2 \hbar^3} \int_{-g_L}^{F_L} [D(\varepsilon_z) + D^2(\varepsilon_z)] (F_L - \varepsilon_z) d\varepsilon_z \quad (39)$$

and the expression for the current becomes

$$I = -\frac{qm}{2\pi^2 \hbar^3} \int_{-g_L}^{F_L} D(\varepsilon_z) (F_L - \varepsilon_z) d\varepsilon_z \quad (40)$$

We note that in this case $S_I(0)$ and I depend on V only through u_L and the direct calculation of the integrals in Eqs. (39) and (40) gives for the Fano factor $\gamma = S_I(0)/(2|qI|)$

$$\gamma(F, u_L) = 1 - \frac{4\Gamma_L \Gamma_R}{\Gamma^2} \frac{A}{B} \quad (41)$$

where

$$A = (f + \xi) \left[\frac{f + \xi}{1 + (f + \xi)^2} + \arctan(f + \xi) - \frac{\xi}{1 + \xi^2} - \arctan(\xi) \right] + \frac{1}{1 + (f + \xi)^2} - \frac{1}{1 + \xi^2}, \quad (42)$$

$$B = 2(f + \xi) [\arctan(f + \xi) - \arctan(\xi)] - \ln \left(\frac{1 + (f + \xi)^2}{1 + \xi^2} \right) \quad (43)$$

here for convenience we have defined dimensionless chemical potential f and voltage drop ξ as

$$f = \frac{2(F_L + g_L)}{\Gamma}, \quad \xi = \frac{2(qu - \varepsilon_r - g_L)}{\Gamma} \quad (44)$$

Since A and B are positive quantities, from Eq. (41) we can see that the suppression of γ below the unity value is controlled by the factor $4\Gamma_L \Gamma_R/\Gamma^2$ which represents the maximum transparency of the double barrier structure.

Figure 2 reports the current (Fig. 2(a)) and the Fano factor (Fig. 2(b)) as function of ξ for different values of f , when $\Gamma_L = \Gamma_R = \Gamma/2$. Curves labelled 1, 2, and 3 correspond to $f = 1, 15$ and ∞ , respectively. The current exhibits the well known peaked behavior and reduces to zero at the highest voltages because we consider only the first resonant level. Of interest is the behavior of the Fano factor reported in Fig. 2(b). The common features of all curves is the presence of a minimum of γ near to the current peak and the evidence of full shot noise in

regions where the current is relatively small. Remarkably, the minimum value of the Fano factor is found to be always less than 0.5, taking the universal value 0.391 at $\xi = -0.801$ for $f \rightarrow \infty$ and being systematically lower than this value at decreasing value of f . More precisely, for $f \rightarrow \infty$ the increase of the current toward the peak is widely broadened in the positive differential conductance region and the value of γ remains close to 0.5 for $\xi < -1$. This corresponds to the case when the resonant level is far from the bottom of the conduction band in the emitter. We notice that the results of Refs. [7] and [32], which are claimed to be related to the coherent tunnel regime, always predict Fano factors greater than or equal to 0.5 contrary to present findings. We believe that the source of the discrepancy comes from the fact that their approaches used to rough an estimation in calculating the average transparency near to the current peak thus underestimating the effect of suppression. By contrast, the theory developed in Ref. [11], making use of a master equation is inherently formulated for a sequential tunneling regime, and thus is not able to catch the essential dynamical feature of the coherent tunnel regime. For $f \rightarrow \infty$, the Fano factor is found to take the universal expression:

$$\gamma(\xi) = 1 - \frac{4\Gamma_L \Gamma_R}{\Gamma^2} \left\{ 1 - \frac{\xi}{(1 + \xi^2) \left[\frac{\pi}{2} - \arctan(\xi) \right]} \right\} \quad (45)$$

An analogous equation was derived by Averin³⁴ for a one dimensional structure. From Fig. 2(b), it is clear that by decreasing the value of f also the minimum of the Fano factor decreases systematically down to a zero value. To understand the physical reason of this behavior, we discuss the limiting condition when $f \ll 1$. In this limit, the width of the electron energy distribution is lower than that of the resonant state. As a consequence, the transmission probability becomes the same for all the electrons and for the Fano factor we obtain the standard partition expression²⁶ $\gamma(\xi) = 1 - D(\xi)$. When $D(\xi)$ is close to unity, γ tends to zero as found by Lesovik³³ for the analogous case of a quantum point contact. Of course, $f \ll 1$ is an ideal condition which is rather difficult to check experimentally in DBRDs, because in this case all the electron flux crosses the structure without undergoing any reflection.

At this point we make one more remark to the results of Ref. [32] and which concerns with the generalization of the formula for the Fano factor in the case of incoherent tunneling. These authors treated the scattering as a simple phase adding during tunneling, thus assuming that an electron does not change its state because of scattering. However, under a real scattering event the electron changes its state and as a consequence it can occupy states in the quantum well belonging to other tunneling states. Thus, a real scattering event destroys the independence of tunneling in different channels and, therefore, the expression for the Fano factor valid for the coherent tunneling becomes no longer valid for the incoherent tunneling. As a result, the way used in Ref. [32] to

derive the Fano factor for incoherent tunneling cannot be applied to real scattering processes. We conclude, that the main reason for shot noise suppression in DBRDs at zero temperature is connected with Pauli principle and, because of the coherent tunneling regime, near to the current peak the Fano factor can take values significantly lower than 0.5.

B. High temperatures

For relatively high temperatures ($T \geq 77$ K), the Coulomb interaction is expected to play a major role in providing deviations of shot noise from its full Poissonian value. To this purpose, we now investigate the effects of the Coulomb interaction in the present coherent approach. We consider the case of high applied voltages when the electron flux from the collector to the emitter can be neglected, the typical condition for the observation of shot noise. In this case, according to Eq. (34) the Coulomb influence on the noise is determined by the value of q_{eff}^+ . We note that the considered range of applied bias can be divided two regions.

The first corresponds to low voltages so that the value qu remains smaller than $(\varepsilon_r + g_L)$ (i.e. the resonant level in the well is above the electron level in the emitter). Then, the number of electrons in the quantum well, N_{QW} , rises with the increase of u_L and $\partial N_{QW}/\partial u_L > 0$. In this voltage region the absolute value of the current rises with the increase of u_L too, but $I < 0$ and so $\partial I/\partial u_L < 0$. As it follows from Eq. (29), $|q_{eff}^+| < 1$ and in this voltage region the Coulomb interaction provides a negative feedback analogously to the shot noise suppression in vacuum diodes³¹.

The second region corresponds to high voltages so that the resonant level remains below that of the electron in the emitter and both N_{QW} and $|I|$ decrease with the increase of u_L . Thus, in this region $\partial N_{QW}/\partial u_L < 0$ and $\partial I/\partial u_L > 0$. Slightly before the instability region, where $(\partial N_{QW}/\partial u_L + C < 0)$, we can see from Eq. (29) that $|q_{eff}^+| > 1$ and there is shot noise enhancement.

We conclude that for coherent tunnelling in DBRDs the Coulomb interaction can suppress and enhance shot noise with respect to the full Poissonian value while Pauli principle can only suppress the shot noise. We remark, that in contrast with the sequential tunneling, where $\gamma \geq 0.5$ ¹¹, in the coherent tunnelling the noise suppression can be much stronger with the Fano factor attaining values much less than 0.5 and even down to zero. It means that giant suppression of shot noise, corresponding to $\gamma < 0.5$, points out that *coherent* tunnelling dominates the current flow in DBRDs.

In the following we study in more details the limiting condition when $k_B T \gg \Gamma$ and $qV > F_L$. Under these conditions, the distribution function slowly varies relatively to the density of states G_{QW} and all integrals over the electron energy can be calculated analytically. For the current and the electron number in the quantum well

we obtain the following expressions

$$I = -q \frac{mT\Gamma_L\Gamma_R}{\pi^2\hbar^3\Gamma} \left[\frac{\pi}{2} - \arctan \left(\frac{2(qu - \varepsilon_r - g_L)}{\Gamma} \right) \right] \rho, \quad (46)$$

with

$$\rho = \ln \left[1 + \exp \left(\frac{F_L - \varepsilon_r + qu}{k_B T} \right) \right] \quad (47)$$

and

$$N_{QW} = -\frac{\hbar}{q\Gamma_R} I \quad (48)$$

By introducing the differential capacitance of the quantum well, $C_{QW} = q\partial N_{QW}/\partial u_L$, q_{eff}^+ can be rewritten in the form

$$q_{eff}^+(\varepsilon) = 1 - \alpha [1 - f_L(\varepsilon)], \quad (49)$$

with $\alpha = C_{QW}/(C + C_{QW})$, and from Eq. (34) we obtain the expression for the Fano factor

$$\gamma = \left[1 - 2\alpha \frac{\beta}{\rho} + \frac{\alpha^2}{\rho} \left(\beta - \frac{1}{2}\beta^2 \right) \right] - \frac{2\Gamma_L\Gamma_R}{\Gamma^2} \left(1 - \frac{\beta}{\rho} \right) \times \\ \left[1 - \frac{\frac{\Gamma}{2}(qu - \varepsilon_r - g_L)}{\left[\frac{\Gamma^2}{4} + (qu - \varepsilon_r - g_L)^2 \right] \left[\frac{\pi}{2} - \arctan \left(\frac{2(qu - \varepsilon_r - g_L)}{\Gamma} \right) \right]} \right] \quad (50)$$

where

$$\beta = \left[1 + \exp \left(\frac{\varepsilon_r - qu - F_L}{k_B T} \right) \right]^{-1} < \rho \quad (51)$$

In equation (50) the terms proportional to α and α^2 are associated with the Coulomb effects and the term proportional to $2\Gamma_L\Gamma_R/\Gamma^2$ is associated with Pauli principle and it corresponds to the term proportional to D^2 in Eq. (34). We note that in the case when the occupation probability of the states in the emitter corresponding to the position of the resonant level is much less than unity (i.e. $\exp \left(\frac{\varepsilon_r - qu - F_L}{k_B T} \right) \gg 1$), $\rho \approx \beta \ll 1$, the electron gas is nondegenerate and

$$\gamma \approx (1 - \alpha)^2 \quad (52)$$

In the opposite case, $\rho \gg \beta$, the electron gas is degenerate, and in Eq. (50) the terms proportional to α and α^2 become negligible. This case recovers the condition of zero temperature discussed in the previous subsection.

From equation (52) it is clear that γ can take values close to zero when α is close to unity. Let us now discuss in detail which parameters define the value of α . According to Eq. (46), α is close to unity when $C_{QW} \gg C$. From equation (25) we see that the value of C is determined by the set of capacitances: C_L , C_R , C_1 , C_2 . We note that

C_R is inversely proportional to the width of the depletion region in the collector. The length of this region increases from the value of the screening length at small voltages to values which, near to the current peak, usually are several times greater than the sum $(d_L + d_{QW} + d_R)$ and so $C_R \ll C_1, C_2$. The value of the capacitance C_L is determined by the accumulation region in the emitter and rises with the increase of the applied voltage. Its value for typical parameters⁸ can be comparable with C_1 . Thus, from Eq. (25) we conclude that to a first estimate $C \approx C_L$. Note that C_L rises with the increase of u_L . On the other hand, from Eq. (45), for a first estimate of the maximum value of C_{QW} we obtain

$$C_{QW}^{max} \approx \frac{q^2 m \Gamma_L}{\pi \hbar^2 \Gamma} \left(1 + \frac{C_L}{C_2} \right) [1 + \exp(-F_L/k_B T)]^{-1} \quad (53)$$

Usually, the maximum shot noise suppression is observed just before the current peak. Under these conditions, the resonant level is aligned with the first quantized level of the emitter. Thus, we conclude that the maximum shot noise suppression due to the Coulomb interaction is determined by the ratio between C_{QW} and C_L near to the current peak.

C. Comparison of theory with experiments

We compare theory with two sets of experiments performed on DBRDs with barriers sufficiently narrow to expect that coherent tunneling Is of importance. The first set refers to pioneer experiments of Brown⁸ which are detailed at 77 K with indications at 4.2 and 300 K. The second set refers to recent experiments at 300 K reported in Ref. [36,37]. In both cases the comparison is limited to the voltage region up to the peak current since theory neglects energy levels higher than the first in the quantum well.

Figure 3 reports the comparison between experiments performed in Ref. [8] at 77 K and the results of present calculations at 77 and 4.2 K. Numerical results make use of the following values for the parameters entering the model: $\varepsilon_r = 104$ meV, $\Gamma_R = \Gamma_L = 0.48$ meV, $n = 2 \times 10^{16}$ cm⁻³, $d_L = d_R = 5 = d_{QW} = 5$ nm, $L = 50$ nm, $m = 0.067 m_0$, with m_0 the free electron mass and $\kappa = 12.9$. The only two fitting parameters are ε_r and $\Gamma = 0.5\Gamma_{L,R}$. Their values control the location and the amplitude of the current peak, respectively, and are chosen by optimizing the agreement between the experimental and the calculated I-V characteristic. All other parameters are provided by the experimental conditions, and we want to stress that the Fano factor is obtained from the same set of parameter values.

The function $g_L(u_L)$ is calculated by solving the Schrödinger equation for a potential which: (i) for $x < 0$ follows from the Poisson equation without accounting for quantization effects; (ii) for $x > 0$ corresponds to the solid solution $Al_{0.42}Ga_{0.58}As$ with zero electric field in-

side, as was done in Ref. [8]. For the used values, the dependence $g_L(u_L)$ is found to be almost linear and well approximated by: $g_L(u_L) \approx 0.44(qu_L - 1.5k_B T) - 0.07k_B T$ for 77 K and $g_L(u_L) \approx 0.28(qu_L - 110k_B T) - 14k_B T$ for 4.2 K. The details of the solution of the Schrödinger equation are reported in the Appendix. From Fig. 3 (a) we see that present calculations well reproduce the current voltage characteristic including the current peak. From Fig. 3 (b) we see that the calculated Fano factor is in satisfactory agreement with the experiments since it reproduces both the suppression and enhanced behaviors. In particular, in the region just before the current peak the observed minimum of the Fano factor is around 0.35, while the calculated value is 0.26. We can explain this disagreement by the fact that most probably not all electrons cross the barriers coherently, so that part of the electron flux follows the sequential tunneling regime. Another probable reason for the disagreement can be the presence of leakage currents. In our opinion both these factors can be responsible for an increase of the noise and thus of the Fano factor. We remark that numerical results at 4.2 K do not differ significantly from those at 77 K in agreement with what claimed by Brown.⁸ Thus, the giant suppression of shot noise at zero temperature predicted by present theory is confirmed by these experiments. In this context, we note that Ref. [16] presented a theoretical calculations of the same experiments⁸ at 77 K. The results of these calculations were found to be in excellent agreement with experimental data except in the region of instability. On the borders of this region the noise tends to infinity, and as a consequence there were no measurements of noise in this region. However, contrary to such an experimental evidence, the theoretical calculations¹⁶ provided finite values of the noise and the absence of the instability region, which makes the theoretical approach at least suspect.

To provide a physical insight of the physical reason for shot-noise suppression, Fig. 4 reports the results of the calculations associated with the "Coulomb" γ_C and the "Pauli" γ_P contributions to the full Poissonian value of the Fano factor according to the relation $\gamma = 1 + \gamma_C + \gamma_P$. From Fig. 4 (a) we see that at 77 K it is the Coulomb part which dominates the shot noise suppression up to the minimum value, and that the Pauli part becomes noticeable near the current peak. Furthermore, while Pauli contribution leads systematically to suppression, the Coulomb contribution becomes responsible of enhanced shot noise at voltages near to 6 V where the instability region is approached. From Fig. 4 (b) the predominance of Pauli over Coulomb effects in suppressing shot noise near zero temperature is confirmed. Again, Coulomb effects are found to be responsible of enhanced shot noise at the current peak in agreement with experiments⁸.

To complete the analysis of this structure at 77 K we have investigated the role played by the electron concentration and the width of the quantum well. Accordingly, Fig. 5 reports the current voltage characteristic

and the Fano factor for the same structure of Fig. 3 but with different values of the electron concentration n in the injector. For the first structure we use $g_L(u_L) \approx 0.37(qu_L - 4k_B T) - 1.79k_B T$ ($n = 2 * 10^{15} \text{ cm}^{-2}$) and for the second $g_L(u_L) \approx 0.22(qu_L - 4k_B T) - 0.09k_B T$ ($n = 2 * 10^{17} \text{ cm}^{-2}$). From the figure it is clear that the increase of n leads to: (i) the increase of the value of the current peak, (ii) the widening of the region of shot noise suppression and, (iii) the decrease of the voltage value corresponding to the current peak and the minimum of the Fano factor. We note that for values of n which differ over two orders of magnitude the peak current changes only for a factor of about 2.5. It means that, due to accumulation, the electron concentration on the border of the left barrier differs only for a factor of 2.5 for voltages corresponding to the current peak. Figure 6 reports the current voltage characteristic and the Fano factor for the same structure of Fig. 3 but with different values of the quantum well width d_{QW} . We have taken into account that when d_{QW} decreases both Γ and ε_r increases by using for the first structure $\varepsilon_r = 145 \text{ meV}$, $\Gamma_L = \Gamma_R = 1 \text{ meV}$ and for the second structure $\varepsilon_r = 45 \text{ meV}$, $\Gamma_L = \Gamma_R = 0.05 \text{ meV}$. This leads to the growth of the current peak and its shift to higher voltages. From the same figure we see that simultaneously with the growth of the current peak also the suppression region width rises and shifts to higher voltages. Remarkably, the minimum value of the Fano factor is found to be practically independent of the electron concentration and of the width of the quantum well considered here.

Figure 7 reports the current voltage characteristic and the Fano factor for the same structure of Fig. 3 at the temperature of 300 K. Here the solution of the Schrödinger equation provides: $g_L(u_L) = 0.53(qu_L - 1.5k_B T) + 0.7k_B T$. We have found that by increasing the temperature the main features of transport and noise already shown at 77 and 4.2 K are preserved. However, the current peak and the minimum of the Fano factor become less pronounced. These trends are in agreement with experimental results⁸ which claim a reduction of the peak-current value of about 1 mA and an increase of the minimum of the Fano factor to a value about 0.45 when going from 77 to 300 K.

A recent set of experiments^{36,37} carried out at 300 K on a DBRD with barriers thinner than those of Ref. [8], thus more adequate to check coherent tunnelling at high temperature, is reported in Fig. 8 together with theoretical calculations. The structure consisted of two 2 nm AlAs layers separated by 6 nm InGaAs quantum well^{35,36}. Measurements were carried out at 300 K using a Noise Figure Meter (XK5-49), that allows to measure simultaneously noise figure and power gain of two-port networks in the 50Ω feed circuit. Simultaneously with the noise the I-V curve was measured. The diode was mounted in the break of a microstrip line, with one electrode been grounded, and another one bonded to the ends of a microstrip line. Noise measurements at frequencies

60 and 200 MHz showed the same results within an experimental uncertainty at worst of 20%, thus indicating that $1/f$ noise contribution is negligible. Numerical results makes use of the following values for the parameters entering the model: $\varepsilon_r = 93 \text{ meV}$, $\Gamma_R = \Gamma_L = 0.9 \text{ meV}$, $n = 7.5 \times 10^{16} \text{ cm}^{-3}$, $d_L = d_R = 2 \text{ nm}$, $d_{QW} = 6 \text{ nm}$, $L = 50 \text{ nm}$, $g_L(u_L) = 0.43(qu_L - 1.5k_B T) + 0.44k_B T$. Also here the only two fitting parameters are ε_r and $\Gamma = 0.5\Gamma_{L,R}$, all other parameters being provided by the experimental conditions, Figure 8(a) reports the I-V characteristics which show a region of positive differential conductance (pdc) up to about 0.7 V followed by an instability region. In the same pdc region, the Fano factor is found to exhibit a suppression with a minimum value of about 0.4 at around 0.6 V [see Fig. 8(b)]. The agreement between theory and experiments is within experimental uncertainty and thus is considered to be satisfactory even in this case. Thus, the comparison between theory and experiments supports the physical interpretation of the giant suppression of shot noise in DBRDs and in particular confirms that coherent transport occurs under such a condition.

VI. CONCLUSIONS

We have carried out a wave-packet approach to investigate DBRDs transport and noise characteristics within the coherent tunnelling regime that includes both Pauli principle and long range Coulomb interaction. In agreement with expectations, theory predicts a current voltage characteristic which exhibits a peak followed by an instability region and that before the current peak shot noise is suppressed because of Pauli principle and/or Coulomb interaction. In addition, theory confirms shot noise enhancement well above the full Poissonian value at the current peak as a consequence of the positive feedback between tunneling and space charge.

At zero temperature, the suppression exhibits a Fano factor of 0.5 in a wide region of applied voltages, with a minimum of 0.391 near the current peak which is experimentally confirmed. Remarkably, the suppression of shot noise below the value 0.5 of the full Poissonian value is found to be a signature of coherent tunneling since sequential tunneling can predict at most suppression with a Fano factor not less than 0.5. At temperatures above about 77 K, we have found that coherent tunneling predicts that shot noise can be suppressed well below the value of 0.5 mostly because of Coulomb interaction. This giant suppression is confirmed by experiments performed at 77 and 300 K.

The reason why shot noise suppression is more effective for coherent than for sequential tunneling can be physically explained as follows. Starting from the fact that the two mechanisms responsible for shot noise suppression are Pauli principle and Coulomb interaction, we note that both act simultaneously for coherent and sequential tunneling. Let us consider the first of them, which is

the most relevant at zero temperature, in the case when the Fermi energy is so small that all the electrons exhibit the same transparency. Coherent transport admits a transparency equal to unity, which implies $\gamma = 1 - D$ according to Lesovik findings³³. For sequential transport the total transparency is always less than unity, since due to scattering an electron can change the direction of motion. As a consequence, under coherent transport for the possible case of full transparency (i.e. $D = 1$) there is no noise; by contrast, under sequential transport the presence of scattering inside the quantum well always introduces noise. This example illustrates why Pauli principle is more efficient in suppressing shot noise under coherent than sequential transport. By considering Coulomb interaction, which is more relevant at higher temperatures, we recall that in the absence of collisions it provides giant shot noise suppression³⁸ as in the vacuum tubes³¹ because electron reflection in this case is due only to Coulomb interaction. It is clear that the presence of scattering provides additional random mechanisms for electrons returning to the emitter and, therefore, provides an additional source of noise. Even this example shows that Coulomb interaction is more efficient in suppressing shot noise under coherent than sequential transport. We finally want to stress that the main reason of the difference between these approaches stems from

the fact that the sequential tunneling is based on a master equation^{11,32} for treating fluctuations of carrier numbers inside the quantum well while coherent tunneling uses the quantum partition noise within the wave-packet approach²⁶. The master equation describes implicitly a sequential mechanism for a carrier entering/exiting from the well and, as a consequence, its intrinsic limit coincides with that of two independent resistors (or vacuum diodes) connected in series and each of them exhibiting full shot noise. This system yields a maximum suppression of shot noise down to the value of 0.5. By contrast, partition noise, inherent to the wave-packet formalism, can be fully suppressed down to zero in the presence of a fully transparent barrier and/or of Coulomb interaction like in vacuum diodes.

ACKNOWLEDGMENTS

We thank Prof. V. Volkov of Moscow Institute of Radioengineering and Electronics for having suggested the problem of this research. Partial support from the Italian Ministry of Foreign Affairs through the Volta Landau Center (the fellowship of V.Ya.A.), and the SPOT-NOSED project IST-2001-38899 of the EC is gratefully acknowledged.

¹ R. Tsu and L. Esaki, *Appl. Phys. Lett.*, **22**, 562 (1973).
² V. Goldman, D. Tsui, and J. Cunningham, *Phys. Rev. Lett.* **58**, 1256 (1987).
³ Y. M. Blanter and M. Büttiker, *Phys. Rep.* **336**, 1 (2000).
⁴ L.L. Chang, L. Esaki and R. Tsui, *Appl. Phys. Lett.*, **24**, 593 (1974).
⁵ S. Luryi, *Appl. Phys. Lett.*, **47**, 490 (1985).
⁶ Y.P. Li, A. Zaslavsky, D.C. Tsui, M. Santos and M. Shayegan, *Phys. Rev. B* **41**, 8388 (1990).
⁷ L.Y. Chen and C.S. Ting, *Phys. Rev. B* **43**, 4534 (1991).
⁸ E.R. Brown, *IEEE Trans on Electron Dev.* **39**, 2686 (1992).
⁹ S. Hershfield, *Phys. Rev. B* **46**, 7061 (1992).
¹⁰ E. Runge, *Phys. Rev. B* **47**, 2003 (1993).
¹¹ G. Iannaccone, M. Macucci and B. Pellegrini, *Phys. Rev. B* **55**, 4539 (1997).
¹² H. B. Sun and G. Milburn, *Phys. Rev. B* **59**, 10748 (1999).
¹³ A. Przadka, K.J. Webb, D.B. Janes, H.C. Liu and Z.R. Wasilewski, *Appl. Phys. Lett.* **71**, 530 (1997).
¹⁴ V. Kuznetsov, E. Mendez, J. Bruno, and J. Pham, *Phys. Rev. B* **58**, R10159 (1998).
¹⁵ J.C. Euges, S. Hershfield and J.V. Wilkins, *Phys. Rev. B* **49**, 13517 (1994).
¹⁶ M. Jahan and A. Anwar, *Solid-State Electron.* **38**, 429 (1995).
¹⁷ L. Chen and C. Ting, *Phys. Rev. B* **46**, 4714 (1992).
¹⁸ J. Davies, P. Hyldgaard, S. Hershfield and J. Wilkins, *Phys. Rev. B* **46**, 9620 (1992).
¹⁹ L. Chen, *Phys. Rev. B* **48**, 4914 (1993).
²⁰ K. Hung and G. Wu, *Phys. Rev. B* **48**, 14687 (1993).
²¹ S. Hershfield, J.H. Davies, P. Hyldgaard, C.J. Stanton and J.W. Wilkins, *Phys. Rev. B* **47**, 1967 (1993).
²² Y. M. Blanter and M. Büttiker, *Phys. Rev. B* **59**, 10217 (1999).
²³ V. Ya. Aleshkin and L. Reggiani, *Phys. Rev. B*, **64**, 245333 (2001).
²⁴ V. Ya. Aleshkin, L. Reggiani and A. Reklaitis, *Phys. Rev. B*, **63**, 085302 (2001).
²⁵ R. Landauer, *Physica D*, **38**, 226 (1987).
²⁶ T. Martin and R. Landauer, *Phys. Rev. B*, **45**, 1742 (1992).
²⁷ L. Landau and E. Lifshiz, *Quantum Mechanics* (Pergamon Press, Oxford, 1977).
²⁸ A.P. Jauho, N.S. Wingreen and Y. Meir, *Phys. Rev. B* **50**, 5528 (1994).
²⁹ N. Ashcroft and N. Mermin, *Solid State Physics* (Holt, Rinehart and Winston, New York, 1976).
³⁰ J.M.L. Figueiredo, C.R. Stanley, A.R. Boyd, C.N. Ironside, S.G. McMeekin and A.M.P. Leite, *Appl. Phys. Lett.* **74**, 1197 (1999).
³¹ A. Van der Ziel: *Noise*, Prentice Hall, New York (1954).
³² J.H. Davies, J.C. Euges and J.W. Wilkins, *Phys. Rev. B* **55**, 11259 (1995).
³³ G.B. Lesovik, *JETP Lett.* **49**, (1989).
³⁴ D.V. Averin, *J. Appl. Phys.* **73**, 2593 (1993).
³⁵ N.V. Alkeev, V.E. Lyubchenko, C.N. Ironside, S.G. McMeekin and A.M.P. Leite, *J. Commun. Technol. Electron.*, **45**, 911 (2000).
³⁶ N.V. Alkeev, V.E. Lyubchenko, C.N. Ironside, J.M.L. Figueiredo and C.R. Stanley, *J. Commun. Technol. Electron.*, **47**, 228 (2002).
³⁷ V. Ya. Aleshkin, L. Reggiani, N.V. Alkeev, V.E. Lyubchenko, C.N. Ironside, J.M.L. Figueiredo and C.R. Stanley, unpublished (2003).

³⁸ G. Gomila, I.R. Cantalapiedra, T. Gonzalez and L. Reggiani, Phys. Rev. B **66**, 75302 (2002).
³⁹ G. Iannaccone, G. Lombardi, M. Macucci and B. Pellegrini, Phys. Rev. Lett. **80**, 1054 (1998).

VII. APPENDIX

Here we detail the calculations to evaluate the differential capacitances of the DBRDs and the solution of the Schrödinger equation for the voltage dependence of the first electron level in the emitter.

A. Capacitances

By recalling that $Q_L = -\kappa\varphi'_L/4\pi$ from Eq. (9) we have

$$C_L(u_L) = q \left\{ N_c F_{1/2} \left(\frac{F_L + qu_L}{k_B T} \right) - n \right\} \sqrt{\frac{\kappa}{8\pi k_B T}} \times \\ \left[N_c F_{3/2} \left(\frac{F_L + qu_L}{k_B T} \right) - N_c F_{3/2} \left(\frac{F_L}{k_B T} \right) - \frac{q}{k_B T} n u_L \right]^{-1/2} \quad (A1)$$

If the electron accumulation is relevant (i.e. $qu_L > k_B T$) then we can write

$$C_L(u_L) \approx q \frac{N_c F_{1/2} \left(\frac{F_L + qu_L}{k_B T} \right)}{\sqrt{\frac{8\pi k_B T}{\kappa\kappa_0} N_c F_{3/2} \left(\frac{F_L + qu_L}{k_B T} \right)}} \quad (A2)$$

By substituting for Q_R the value given in Eq. (13), for C_R we find

$$C_R = q \left\{ n - N_c F_{1/2} \left(\frac{F_L + qu_L - qV}{k_B T} \right) \right\} \sqrt{\frac{\kappa}{8\pi k_B T}} \\ \left[N_c F_{3/2} \left(\frac{F_L + qu_R - qV}{k_B T} \right) - N_c F_{3/2} \left(\frac{F_L - qV}{k_B T} \right) \right. \\ \left. - \frac{qn}{k_B T} (u_R - V) \right]^{-1/2} \quad (A3)$$

If $q(V - u_R)/(k_B T) > 1$, then we have the usual expression for the capacitance of the depletion region

$$C_R \approx \sqrt{\frac{q\kappa n}{8\pi(V - u_R)}} \quad (A4)$$

B. Energy of the first electron level in the emitter

The one dimensional Schrödinger equation for an electron moving in the potential $-q\varphi(x)$ can be written in the following form

$$\frac{dy}{dx} + y^2 + \frac{2m}{\hbar^2} (q\varphi + \varepsilon) = 0 \quad (B1)$$

here $y = \Psi'/\Psi$, Ψ is the electron wave function and ε the electron energy. Since $d\varphi/dx$ in the emitter is function of φ [see Eqs. (8) and (9)], instead of x it is convenient to use φ as variable quantity so that

$$\frac{dy}{d\varphi} \frac{d\varphi}{dx} + y^2 + \frac{2m}{\hbar^2} (q\varphi + \varepsilon) = 0 \quad (B2)$$

where

$$\frac{d\varphi}{dx} = \sqrt{\frac{8\pi k_B T}{\kappa}} \left[N_c F_{3/2} \left(\frac{F_L + q\varphi}{k_B T} \right) - N_c F_{3/2} \left(\frac{F_L}{k_B T} \right) \right. \\ \left. - \frac{q}{k_B T} n \varphi \right]^{1/2} \quad (B3)$$

The potential φ in the emitter takes values in the range from 0 far from the barriers ($x \rightarrow -\infty$) to u_L on the border of the left barrier. We note that far from the barriers the potential falls exponentially $\varphi \sim \exp(x/\lambda_D)$ when $q\varphi \ll k_B T$, where λ_D is the Debye screening length. For localized state the electron wave function $\Psi \sim \exp(k_1 x)$ for $x \rightarrow -\infty$, where $k_1 = \sqrt{-2m\varepsilon/\hbar}$ and, thus, we have as boundary condition $y(\varphi = 0) = k_1$. Since we suppose that the field in the barrier is absent, the electron wave function in the barrier is $\Psi \sim \exp(-k_2 x)$ where $k_2 = \sqrt{2m(\Delta E_c - qu_L - \varepsilon)/\hbar}$ and ΔE_c is the conduction band offset on the barrier border. By using the conditions of continuity of the wave function and of its derivative, we obtain the second boundary condition $y(\varphi = u_L) = -k_2$. Equations (B2) and (B3) together with the boundary conditions allow us to find the energy of the first electron level in the potential well of the emitter by numerical calculations.

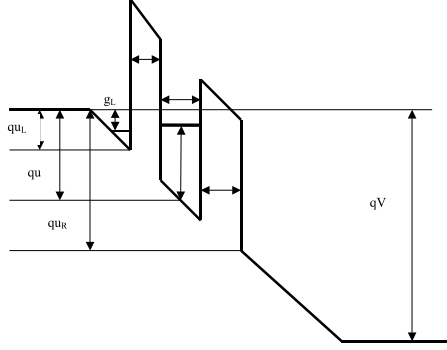


FIG. 1: Sketch of the band profile of the double barrier structure. The bottom of the conduction band in the emitter in the well and in the collector coincides at $V = 0$

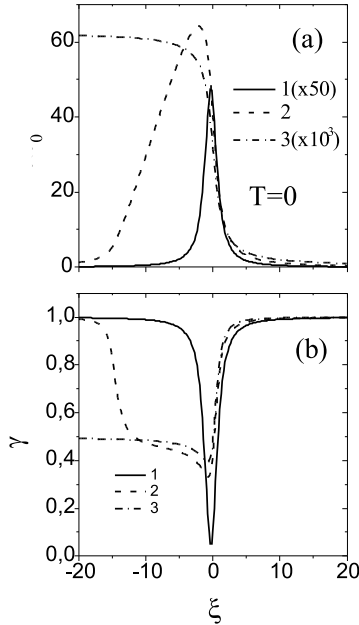


FIG. 2: Dependence of the Fano factor and of the dimensionless current on the dimensionless electrical potential $\xi = 2(qu - \varepsilon_r - g_L)/\Gamma$. Curves 1, 2, and 3 correspond, respectively, to dimensionless chemical potentials $f = 1, 15, \infty$. Here $f = 2(F_L + g_L)/\Gamma$ and $I_0 = qm\Gamma_L\Gamma_R/(2\pi^2\hbar^3)$.

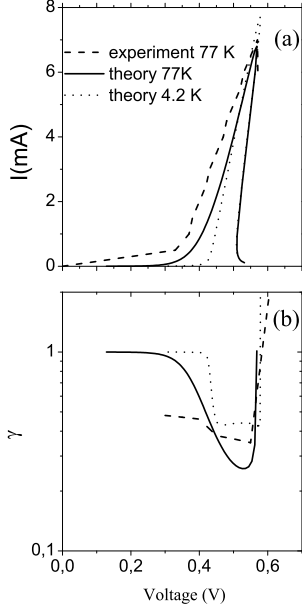


FIG. 3: Experimental and calculated dependencies of current (a) and Fano factor (b) on applied voltage for the structure in Ref. [8]. Experiments refer to $T = 77$ K and theory to $T = 4$ and 77 K, respectively.

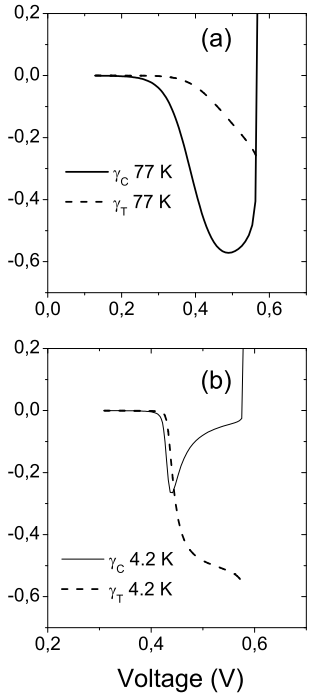


FIG. 4: Dependencies of "Coulomb" γ_C and "Pauli" γ_T contributions to the full Poissonian value of the Fano factor, $\gamma = 1 + \gamma_C + \gamma_T$, on applied voltage at 4 K (a) and 77 K (b), respectively.

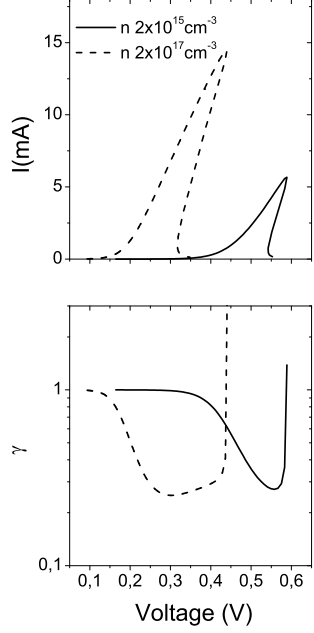


FIG. 5: Dependencies of current and Fano factor on applied voltage for structures with $n = 2 \times 10^{15} \text{ cm}^{-3}$ (solid) and $n = 2 \times 10^{17} \text{ cm}^{-3}$ (dashed). Other parameters are as in Fig. 3.

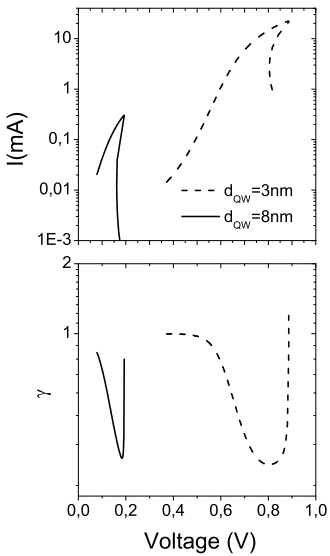


FIG. 6: Dependencies of current and Fano factor on applied voltage for structures with $d_{QW} = 3 \text{ nm}$ (dashed curve) and $d_{QW} = 8 \text{ nm}$ (solid curve). For the first structure we used $\varepsilon_r = 145 \text{ meV}$, $\Gamma_L = \Gamma_R = 1 \text{ meV}$. For the second structure we used $\varepsilon_r = 45 \text{ meV}$, $\Gamma_L = \Gamma_R = 0.05 \text{ meV}$. Other parameters are as in Fig. 3

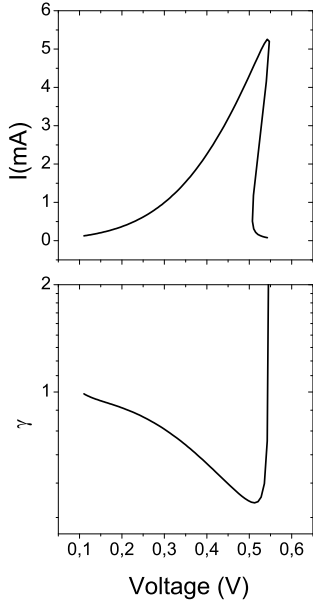


FIG. 7: Dependencies of current and Fano factor on applied voltage at $T = 300\text{ K}$. Other parameters are as in Fig. 3.

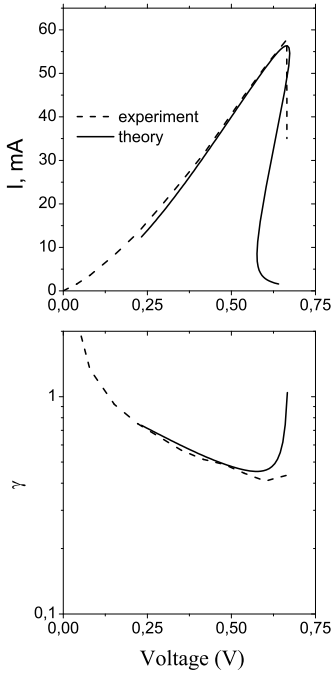


FIG. 8: Experimental and calculated dependencies of current (a) and Fano factor (b) on applied voltage for the structure in Ref. [36,37] at $T = 300\text{ K}$.